

Gravitational waves from a first-order phase transition: sound waves and turbulence

11th LISA Cosmology Working Group Workshop
Jun. 18, 2024



Alberto Roper Pol
University of Geneva



SNSF Ambizione grant: *“Exploring the early universe with gravitational waves
and primordial magnetic fields”*

Collaborators: A. Brandenburg (Nordita), T. Boyer (APC), C. Caprini (UniGe/CERN), R. Jinno (Kobe),
T. Kahniashvili (CMU), T. Konstandin (DESY), A. Kosowsky (PittU),
S. Mandal (CMU), A. S. Midiri (UniGe), A. Neronov (APC/EPFL),
S. Procacci (UniGe), H. Rubira (TUM), I. Stomberg (DESY), D. Semikoz (APC)

arXiv: 1903.08585, 2009.14174, 2201.05630, 2307.10744, **2308.12943**

<https://github.com/AlbertoRoper/cosmoGW> [CosmoGW]

Cosmological GW background

The observation of a cosmological GW background would provide us with *direct information on early universe physics* that is *not accessible via electromagnetic observations, possibly complementary to collider experiments*:

nature of first-order phase transitions
(baryogenesis, BSM physics, high-energy physics),
primordial origin of intergalactic magnetic fields.

Probing the early Universe with GWs

Cosmological (pre-recombination) GW background

- Why background? Individual sources are not resolvable, superposition of single events occurring in the whole Universe.

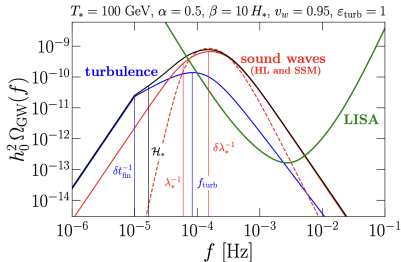
$$f_* \simeq 1.64 \times 10^{-3} \frac{100}{R_* \mathcal{H}_*} \frac{T_*}{100 \text{ GeV}} \text{ Hz}$$

- Phase transitions
 - Ground-based detectors (LVK, ET, CE) frequencies are 10–1000 Hz
Peccei-Quinn, B-L, left-right symmetries $\sim 10^7, 10^8$ GeV.
 - Space-based detectors (**LISA**) frequencies are 10^{-5} – 10^{-2} Hz
Electroweak phase transition ~ 100 GeV
 - Pulsar Timing Array (PTA) frequencies are 10^{-9} – 10^{-7} Hz
Quark confinement (QCD) phase transition ~ 100 MeV

GW sources in the early universe

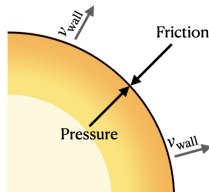
- Magnetohydrodynamic (MHD) sources of GWs:
 - Sound waves generated from first-order phase transitions.
 - Primordial magnetic fields.
 - (M)HD turbulence from first-order phase transitions.
- High-conductivity of the early universe leads to a high-coupling between magnetic and velocity fields.
- Other sources of GWs include
 - Bubble collisions.
 - Cosmic strings.
 - Primordial black holes.
 - Inflation.

ARP *et al.*, 2307.10744, 2308.12943,
[LISA CosWG] (incl. ARP), arXiv:2403.03723



Hydrodynamics of first-order phase transitions¹

- Broken-phase bubbles are nucleated and expand
- Friction from particles yield a terminal velocity ξ_w of the bubbles
- The bubble can run away when the friction is not enough to stop the bubble's acceleration



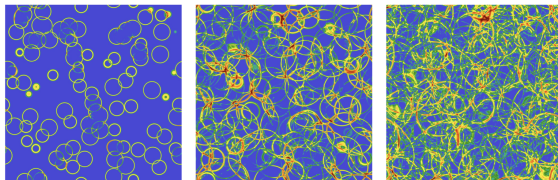
$$\nabla_{\mu} T_{\text{field}}^{\mu\nu} = \frac{\partial V}{\partial \phi} \partial^{\nu} \phi + \eta u^{\mu} \partial_{\mu} \phi \partial^{\nu} \phi,$$

$$\nabla_{\mu} T_{\text{fluid}}^{\mu\nu} = -\frac{\partial V}{\partial \phi} \partial^{\nu} \phi - \eta u^{\mu} \partial_{\mu} \phi \partial^{\nu} \phi,$$

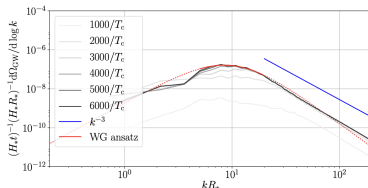
¹Espinosa, Konstandin, No, Servant, *JCAP* **06** (2010) 028.

GWs from sound waves²

- Numerical simulations of the scalar + fluid system can be performed including an effective friction term



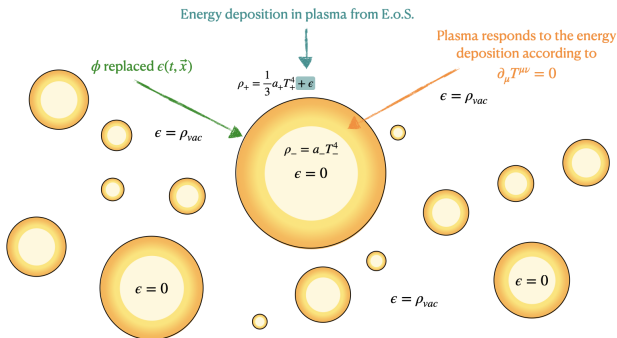
- Two scales are found that determine the GW spectrum: R_* and ΔR_* (sound-shell thickness).



(b) Intermediate, $v_w = 0.92$

GWs from sound waves: Higgsless simulations³

- Difficulty on simulations is due to the different scales of the scalar field ϕ and the fluid shell, so one can consider a nucleation history and set the pressure and energy density by knowing the value of ϵ and setting it during the simulation.
- Effect of bubble collisions on GWs is subdominant when sound waves are produced, so one can ignore the scalar field.



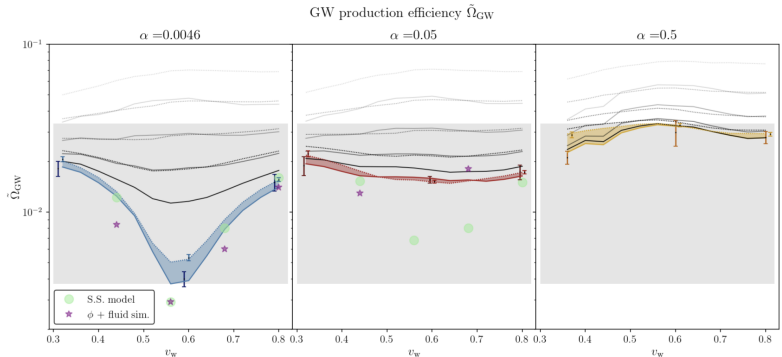
Credit: I. Stomberg

Higgsless simulations: New results **[unpublished]**⁴

- In the literature, based on analytical considerations, the GW spectrum from sound waves is usually assumed to be

$$\Omega_{\text{GW}}(f) = 3 \tilde{\Omega}_{\text{GW}} K^2 (H_* \tau_{\text{SW}}) (H_* R_*) S(f R_*)$$

- $\tilde{\Omega}_{\text{GW}}$ is the efficiency factor

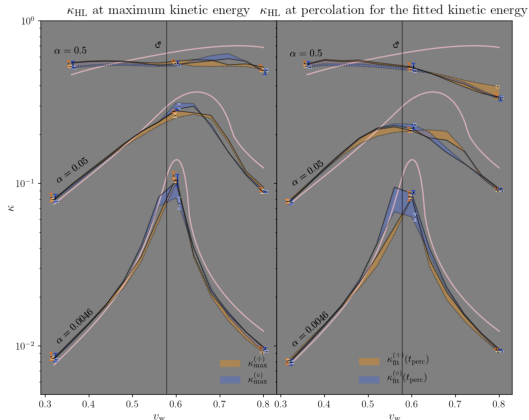


Higgsless simulations: New results **[unpublished]**⁵

- In the literature, based on analytical considerations, the GW spectrum from sound waves is usually assumed to be

$$\Omega_{\text{GW}}(f) = 3 \tilde{\Omega}_{\text{GW}} K^2 (H_* \tau_{\text{SW}}) (H_* R_*) S(f R_*)$$

- $K \equiv \kappa \alpha / (1 + \alpha)$ is the fraction of kinetic (in the sound-wave regime!) to radiation energy density



Analytical computation of the GW spectrum

- The GW spectrum at present time produced by the anisotropic stresses $\Pi_{ij} = T_{ij}^{\text{TT}}/\rho_{\text{tot}}$ active in a finite time interval $\tau \in (\tau_*, \tau_{\text{fin}})$, ignoring the expansion of the Universe, is

$$\Omega_{\text{GW}}(f) = \frac{3}{4\pi^2} \mathcal{T}_{\text{GW}} k^3 H_*^2 \int_{\tau_*}^{\tau_{\text{fin}}} \int_{\tau_*}^{\tau_{\text{fin}}} dt_1 dt_2 \cos k(t_1 - t_2) P_{\Pi}(k, t_1, t_2)$$

- During radiation-domination with $a \sim \tau$, including the effect of the expansion of the Universe,

$$\Omega_{\text{GW}}(f) = \frac{3}{4\pi^2} \mathcal{T}_{\text{GW}} k^3 \int_{\tau_*}^{\tau_{\text{fin}}} \int_{\tau_*}^{\tau_{\text{fin}}} \frac{dt_1 dt_2}{t_1 t_2} \cos k(t_1 - t_2) P_{\Pi}(k, t_1, t_2)$$

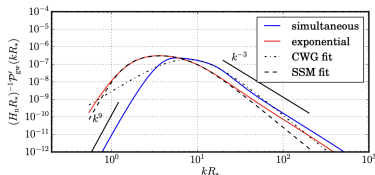
- P_{Π} is the unequal-time correlator (UETC) of the source and it usually requires to be evaluated under a specific model for analytical computations.

GWs from sound waves: Sound Shell Model⁶

- The sound shell model assumes linear superposition of velocity fields from each of the single bubbles and averages over nucleation locations and bubbles lifetimes (semi-analytical model), and the development of sound waves at the time of collisions. It assumes stationary UETC $P_{\Pi} = P_{\Pi}(k, t_2 - t_1)$.

$$\Omega_{\text{GW}}(f) = 3 \tilde{\Omega}_{\text{GW}} K^2 (H_* \tau_{\text{sw}}) (H_* R_*) S(f R_*)$$

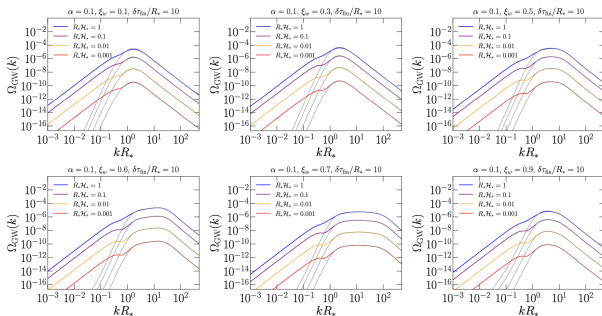
- It predicted a steep k^9 spectrum and linear growth with time, according to HH19, and k^{-3} at large frequencies, with an intermediate k between $1/R_*$ and $1/\Delta R_*$.
- GW predictions usually assume $\tau_{\text{sw}} = \min(\tau_{\text{sh}}, H_*^{-1})$, with $\tau_{\text{sh}} \sim R_*/\sqrt{K}$ being the expected time to develop non-linearities (should be a conformal time interval $\tau_{\text{sw}} = \tau_{\text{fin}} - \tau_*$ due to the conformal invariance of the fluid equations!).



(b) Intermediate, $v_w = 0.92$

GWs from sound waves: Sound Shell Model revisited⁷

- Extended Sound Shell model to an expanding Universe and omitted assumptions that were not holding at small k . Furthermore, an additional contribution to the GW spectrum is identified, omitted in previous studies.
- Recovered k^3 at small frequencies and found a $\ln^2(1 + \tau_{\text{SW}} H_*)$ time evolution of the causal branch and the “linear-in-time” evolution $\Upsilon = \tau_{\text{SW}} H_*/(1 + \tau_{\text{SW}} H_*)$ around the peak, as well as a sharp bump.



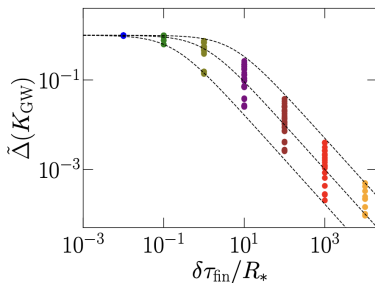
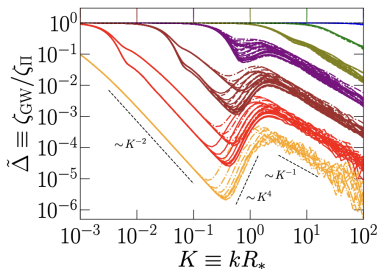
GWs from sound waves: Sound Shell Model revisited⁸

- We show how stationary processes present both regimes and the linear growth is only found when $k \gg 1/\tau_{\text{sw}}$.

$$\Omega_{\text{GW}}(f) = 3 \tilde{\Omega}_{\text{GW}} K^2 \ln^2(1 + \tau_{\text{sw}} H_*) (f R_*)^3 \tilde{\Delta}(f, R_*, \tau_{\text{sw}}) \zeta_{\Pi}(f R_*),$$

where $\zeta_{\Pi}(f) = P_{\Pi}(f, t_1 = t_2 = t_*)/P_{\Pi}(0)$.

- The function $\tilde{\Delta}$ represents the ratio of the normalized GW spectrum to the normalized anisotropic stress spectrum P_{Π} and requires numerical evaluation. At the peak of the GW spectrum, it is roughly constant when $\tau_{\text{sw}} \ll R_*$ and it becomes $\tilde{\Delta} \sim R_*/\tau_{\text{sw}} \sim \sqrt{K}$ when $\tau_{\text{sw}} \gg R_*$.



Computing P_{Π} for irrotational flows [unpublished]⁹

- P_{Π} describes two-point correlations of the stress tensor $P_{\Pi} \sim \langle T_{ij}(\mathbf{x})T_{ij}(\mathbf{y}) \rangle$, hence four-point correlations of the velocity field $P_{\Pi} \sim \langle v_i v_j(\mathbf{x})v_i v_j(\mathbf{y}) \rangle$.
- Applying Wick's theorem,

$$P_{\Pi}(k) \sim \int_0^{\infty} p^2 P_v(p) dp \int_{-1}^1 (1-x^2)^2 \frac{P_v(\tilde{p})}{\tilde{p}^4} dx,$$

where $\tilde{p}^2 = p^2 + k^2 - 2pkx$ and $P_v(k)$ is the spectral density of the velocity field.

- We find that in the phase of expanding bubbles, applying Wicks' theorem leads to the wrong conclusion that $P_{\Pi}(k) \neq 0$. This is due to the fact that the velocity field induced by expanding bubbles does not follow a Gaussian distribution.

Computing P_{Π} for irrotational flows [unpublished]¹⁰

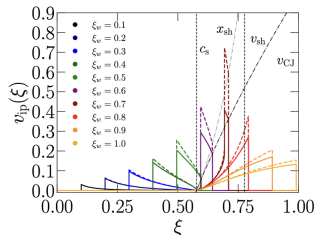
- In the sound-wave regime, we expect that the superposition of many bubbles makes the velocity field statistically Gaussian. Then, using the sound-shell model,

$$P_v(k) \sim \int_0^\infty dT \nu(T) T^6 f'^2(Tk/\beta), \quad f'(z) = -4\pi \int_0^\infty j_1(z\xi) \xi^2 v_{ip}(\xi) d\xi,$$

with $\xi = r/t$ and v_{ip} being the self-similar radial distance to the center of the bubble and the velocity induced by the bubble.

- The generalized Riemann-Lebesgue lemma allows us to compute the asymptotic limit $f'(z \rightarrow \infty)$ based on the discontinuities of $v_{ip}(\xi)$

$$\lim_{z \rightarrow \infty} f'^2(z) = \frac{16\pi^2}{z^4} [\xi_w(v_+ - v_-) + \xi_{sh} v_{sh}^-]^2.$$



Conclusions

- Velocity fields induced by expanding and colliding bubbles in the early universe can significantly contribute to the stochastic GW background (SGWB) via sound waves and (M)HD turbulence (see extra slides).
- The non-linear fluid dynamics requires, in general, performing high-resolution numerical simulations, as done by the Helsinki and the DESY groups using in-house codes, and by the Nordita and Geneva groups using the open-source `PENCIL CODE` for vortical and acoustic turbulence.
- Since the SGWB is a superposition of different sources, it is extremely important to characterize the different sources, to be able to extract clean information from the early universe physics.
- Numerical simulations are crucial to provide insights on the theoretical understanding and on the development of an analytical framework to provide useful and accurate templates for LISA.
- The interplay between sound waves and the development of turbulence is not well understood. It plays an important role on the relative amplitude of both sources of GWs.



Thank You!



alberto.roperpol@unige.ch

github.com/AlbertoRoper/cosmoGW
cosmology.unige.ch/users/alberto-roper-pol





Numerical simulations of early Universe sources of gravitational waves

28 de julio de 2025 a 15 de agosto de 2025 — Albano Building 3

Introduzca su término de búsqueda 🔍

[Main Page](#)

[Campus map](#)

[Practical Information](#)

- [What is Nordita?](#)
- [Directions to Nordita](#)
- [Directions to BizApartment Hotel](#)
- [Nordita Contact Information](#)
- [Tourist Tips](#)
- [Stockholm Tourist Info](#)
- [Stockholm Public Transport](#)

Venue

Nordita, Stockholm, Sweden

organized together with Caprini, Drew, Figueroa, Weir

Scope

The main objectives of the program are:

- to study the different possible sources contributing to the cosmological GW background,
- to review the state-of-the-art numerical codes and techniques in the literature.

For this purpose, the program is divided into four weeks, covering the following potential sources of GWs in the early Universe:

1. Inflation and (p)reheating
2. Scalar perturbations and primordial black holes
3. First order phase transitions and primordial turbulence
4. Topological defects: cosmic strings and domain walls

CosmoGW (<https://github.com/AlbertoRoper/cosmoGW>)

stable version with updated libraries available by the end of 2024!!

- Python toolkit (previously GW_turbulence, <https://zenodo.org/record/6045844>, v.11.02.22)
- Contains python libraries to generate results related to the production of cosmological GW backgrounds and early Universe physics.
- Separate and independent library that can read the results from Pencil Code simulations for post-processing with Python.
- Jupyter notebooks available to reproduce results and with tutorials available for interferometry and cosmology.

GWs from (M)HD turbulence

- Direct numerical simulations using the PENCIL CODE¹¹ to solve:
 - ① Relativistic MHD equations adapted for radiation-dominated era (after electroweak symmetry is broken).
 - ② Gravitational waves equation.
- In general, large-resolution simulations are necessary to solve the MHD nonlinearities (e.g., unequal-time correlators UETC and non-Gaussianities, which require simplifying assumptions in analytical studies).

¹¹Pencil Code Collaboration, JOSS **6**, 2807 (2020), <https://github.com/pencil-code/>
ARP *et al.*, *Geophys. Astrophys. Fluid Dyn.* **114**, 130 (2020).

Conservation laws for MHD turbulence

$$T^{\mu\nu}{}_{;\nu} = 0, \quad F^{\mu\nu}{}_{;\nu} = -J^\mu, \quad \tilde{F}^{\mu\nu}{}_{;\nu} = 0$$

In the limit of subrelativistic bulk flow:

$$\gamma^2 \sim 1 + (v/c)^2 + \mathcal{O}(v/c)^4$$

Relativistic MHD equations are reduced to¹²

$$\frac{\partial \ln \rho}{\partial t} = -\frac{4}{3} (\nabla \cdot \mathbf{u} + \mathbf{u} \cdot \nabla \ln \rho) + \frac{1}{\rho} [\mathbf{u} \cdot (\mathbf{J} \times \mathbf{B}) + \eta J^2],$$

$$\begin{aligned} \frac{D\mathbf{u}}{Dt} = & \frac{1}{3} \mathbf{u} (\nabla \cdot \mathbf{u} + \mathbf{u} \cdot \nabla \ln \rho) - \frac{\mathbf{u}}{\rho} [\mathbf{u} \cdot (\mathbf{J} \times \mathbf{B}) + \eta J^2] \\ & - \frac{1}{4} \nabla \ln \rho + \frac{3}{4\rho} \mathbf{J} \times \mathbf{B} + \frac{2}{\rho} \nabla \cdot (\rho \nu \mathbf{S}), \end{aligned}$$

$$\frac{\partial \mathbf{B}}{\partial t} = \nabla \times (\mathbf{u} \times \mathbf{B} - \eta \mathbf{J}), \quad \mathbf{J} = \nabla \times \mathbf{B},$$

for a flat expanding universe with comoving and normalized

$\rho = a^4 \rho_{\text{phys}}, \rho = a^4 \rho_{\text{phys}}, B_i = a^2 B_{i,\text{phys}}, u_i$, and conformal time t ($dt = a dt_c$).

¹²A. Brandenburg, et al., *Phys. Rev. D* **54**, 1291 (1996).

Numerical results for decaying MHD turbulence¹³

Initial conditions

- Initial stochastic magnetic or (purely vortical) velocity field.

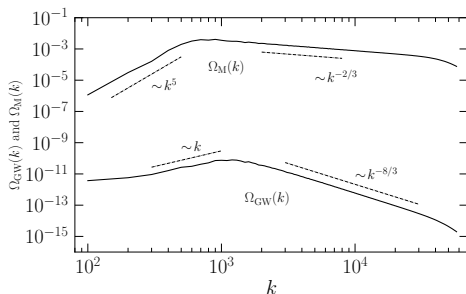
$$kB_i(\mathbf{k}) = \left(\delta_{ij} - \hat{k}_i \hat{k}_j \right) g_j \sqrt{2\Omega_M(k)/k}$$

- Batchelor spectrum for magnetic (or vortical velocity) fields, i.e., $\Omega_M(k) \equiv d\rho_M/d \ln k \propto k^5$ for small $k < k_* \sim \mathcal{O}(\xi_M^{-1})$.
- Kolmogorov spectrum in the inertial range, i.e., $\Omega_M \propto k^{-2/3}$.

¹³ A. Brandenburg *et al.* (incl. ARP), *Phys. Rev. D* **96**, 123528 (2017).
ARP *et al.*, *Phys. Rev. D* **102**, 083512 (2020).
ARP *et al.*, *JCAP* **04** (2022), 019.
ARP *et al.*, *Phys. Rev. D* **105**, 123502 (2022).

Numerical results for decaying MHD turbulence¹⁴

$$1152^3, k_* = 2\pi \times 100, \Omega_M \sim 10^{-2}, \sigma_M = 1$$



- **Characteristic k scaling in the subinertial range for the GW spectrum.**
- k^2 expected at scales $k < k_*$ and k^3 at $k < H_*$ according to the “top-hat” model (Caprini *et al.*, 2020).

Analytical model for GWs from decaying turbulence

- Assumption: magnetic or velocity field evolution $\delta t_e \sim 1/(u_* k_*)$ is slow compared to the GW dynamics ($\delta t_{\text{GW}} \sim 1/k$) at all $k \gtrsim u_* k_*$.
- We can derive an analytical expression for nonhelical fields of the envelope of the oscillations¹⁵ of $\Omega_{\text{GW}}(k)$.

$$\Omega_{\text{GW}}(k, t_{\text{fin}}) \approx 3 \left(\frac{k}{k_*} \right)^3 \Omega_{\text{M}}^*{}^2 \frac{\mathcal{C}(\alpha)}{\mathcal{A}^2(\alpha)} p_{\Pi} \left(\frac{k}{k_*} \right) \\ \times \begin{cases} \ln^2[1 + \mathcal{H}_* \delta t_{\text{fin}}] & \text{if } k \delta t_{\text{fin}} < 1, \\ \ln^2[1 + (k/\mathcal{H}_*)^{-1}] & \text{if } k \delta t_{\text{fin}} \geq 1. \end{cases}$$

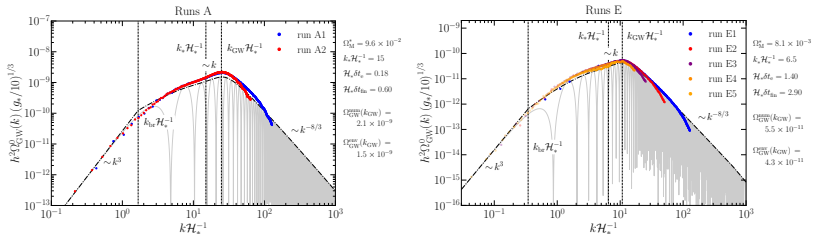
- p_{Π} is the anisotropic stress spectrum and depends on spectral shape, can be approximated for a von Kármán spectrum as¹⁶

$$p_{\Pi}(k/k_*) \simeq \left[1 + \left(\frac{k}{2.2k_*} \right)^{2.15} \right]^{-11/(3 \times 2.15)}$$

¹⁵ ARP et al., *Phys. Rev. D* **105**, 123502 (2022).

¹⁶ ARP et al., arXiv:2307.10744 (2023).

Numerical results for nonhelical decaying MHD turbulence¹⁷



run	Ω_M^*	$k_* \mathcal{H}_*^{-1}$	$\mathcal{H}_* \delta t_e$	$\mathcal{H}_* \delta t_{fin}$	$\Omega_{GW}^{2,0}(k_{GW})$	$[\Omega_{GW}^{2,0}/\Omega_{GW}^{2,0}](k_{GW})$	n	$\mathcal{H}_* L$	$\mathcal{H}_* t_{end}$	$\mathcal{H}_* \eta$
A1	9.6×10^{-2}	15	0.176	0.60	2.1×10^{-9}	1.357	768	6π	9	10^{-7}
A2	-	-	-	-	-	-	768	12π	9	10^{-6}
E1	8.1×10^{-3}	6.5	1.398	2.90	5.5×10^{-11}	1.184	512	4π	8	10^{-7}
E2	-	-	-	-	-	-	512	10π	18	10^{-7}
E3	-	-	-	-	-	-	512	20π	61	10^{-7}
E4	-	-	-	-	-	-	512	30π	114	10^{-7}
E5	-	-	-	-	-	-	512	60π	234	10^{-7}

Primordial turbulence constraints with EPTA DR 2¹⁸

